International Journal of Refrigeration 160 (2024) 88–94

Contents lists available at ScienceDirect

International Journal of Refrigeration

journal homepage: www.elsevier.com/locate/ijrefrig

Thermal conductivity measurements for trans-1,3,3,3-Tetrafluoropropene (R1234ze(E)) in liquid phase

Mesurages de la conductivité thermique du trans-1,3,3,3-Tétrafluoropropène (R1234ze(E)) en phase liquide

Davide Menegazzo [a,b,*], Giulia Lombardo [a,b], Mauro Scattolini [a], Giovanni Ferrarini [a], Stefano Rossi [a], Laura Fedele [a], Sergio Bobbo [a]

[a] Construction Technologies Institute - National Research Council, corso Stati Uniti 4 Padova, 35127, PD, Italy
[b] Department of Industrial Engineering - University of Padova, via Venezia Padova, 35131, PD, Italy

ARTICLE INFO

Keywords:
Low-GWP refrigerants
Thermal conductivity
Hydrofluoroolefins

Mots clés:
Frigorigènes à faible PRP
Conductivité thermique
Hydrofluoroléfines

ABSTRACT

International regulations, such as the European Regulation EU No 517/2014, are pushing the refrigeration, heat pumps and air conditioning sectors to find suitable low-GWP working fluids as alternatives to the currently widespread high-GWP refrigerants, such as R134a and R410A. Halogenated olefins (HFOs and HCFOs) have been considered promising and, among these, trans-1,3,3,3-tetrafluoropropene (R1234ze(E)) has been identified as a potential alternative to R134a in medium temperature applications, including air-cooled and water-cooled chillers, heat pumps, refrigerators and combined with CO_2 in cascade systems. The thermodynamic properties of R1234ze(E) have been widely studied in the last decade. Instead, a comprehensive experimental knowledge on the transport properties of R1234ze(E) is still missing. In order to increase the available experimental transport property data, the present study reports thermal conductivity measurements carried out with a new transient hot-wire (THW) apparatus on R1234ze(E) in the liquid phase at temperatures from 243 K to 343 K and pressure up to 8 MPa. The reported uncertainty is estimated to be lower than 2% and the measurements resulted in agreement with the available literature data.

1. Introduction

In the recent years, the refrigeration, heat pumps and air conditioning sectors have pushed the research for new environmental friendly fluids. This was mainly due to the restrictions imposed by international regulations, such as the Kigali Amendment to the Kyoto Protocol (United Nations Environment Programme, 2016) and EU F-Gas Regulation (European Commission, 2014), whose purpose is to gradually phase-down the working fluids characterized by high Global Warming Potential (GWP) values. The regulations also defined as long-term refrigerants those fluids with GWP lower than 150 (hereafter referred to as low-GWP refrigerants). R134a and R410 A are the market leaders in the refrigeration, air conditioning and heat pumps industries and they are characterized by GWP values of 1530 and 2256 respectively (IPCC, 2021). Thus there is a urgent need to find suitable low-GWP alternatives for both. However, the simple replacement of a high-GWP refrigerant with a low-GWP alternative is not enough to reduce the overall environmental impact of a refrigerating device if the substitution leads to worse performance, and thus increases the indirect emissions (Makhnatch and Khodabandeh, 2014). The replacement of high-GWP refrigerants is challenging because, other than good working performance, the alternatives are required to meet several other criteria, such as stability in the systems, low flammability, low toxicity, but also the price and the market availability narrow the search (Bobbo et al., 2018). McLinden et al. (2014) identified halogenated olefins, i.e. hydrofluoroolefins (HFOs) and hydrochlorofluoroolefins (HCFOs), as the last group of synthetic fluids that can meet the aforementioned requirements. The only alternatives to HFOs and HCFOs are natural refrigerants, such as hydrocarbons, carbon dioxide and ammonia, whose thermophysical properties are not suitable for a number of applications, besides the safety issues due to the high flammability of hydrocarbons and the toxicity of ammonia (Fedele et al., 2023).

Among HFOs, trans-1,3,3,3-tetrafluoropropene (R1234ze(E)) has been considered one of the most promising alternatives to R134a for medium temperature applications, either as pure fluid or blended

* Corresponding author at: Construction Technologies Institute - National Research Council, corso Stati Uniti 4 Padova, 35127, PD, Italy.
E-mail address: menegazzo@itc.cnr.it (D. Menegazzo).

https://doi.org/10.1016/j.ijrefrig.2024.02.004
Received 11 October 2023; Received in revised form 30 January 2024; Accepted 3 February 2024
Available online 19 February 2024

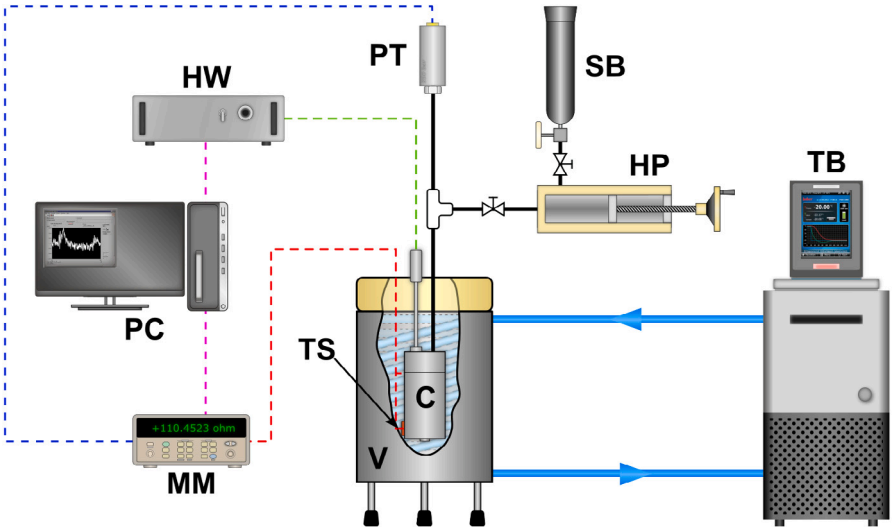

Fig. 1. Scheme of the THW apparatus, consisting of multimeter (MM), Hot Wire controller/data reader (HW), computer (PC), pressure cell (C), thermometer (TS), pressure transducer (PT), pressure vessel (V), sample bottle (SB), handpump (HP) and thermostatic bath (TB).

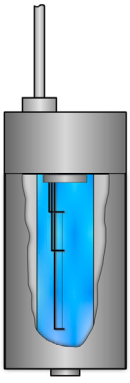

Fig. 2. Detailed view of the pressure cell.

(Mota-Babiloni et al., 2016). R1234ze(E) has been studied as working fluid also for Organic Rankine Cycle (Invernizzi et al., 2016) and high temperature heat pumps (Kondou and Koyama, 2015). The thermophysical properties of R1234ze(E) have been widely studied, while a limited amount of transport properties data is available (Fedele et al., 2023). Concerning the thermal conductivity, three data sets are available in the literature for R1234ze(E). Grebenkov et al. (2009) measured 94 points ranging from 254 K and 407 K and pressures up to 20 MPa. Perkins and Huber (2011) measured 452 points in the temperature range between 203 K and 343 K with pressures up to 23 MPa. Miyara et al. (2011) measured 24 points from 283 K to 353 K at saturation pressure. Moreover, the data from Perkins and Huber (2011) were employed to develop the Extended Corresponding State (ECS) model implemented in Refprop 10.0 (Lemmon et al., 2018) the forecast the thermal conductivity of R1234ze(E).

The present work is aimed to increase the available set of thermal conductivity data for R1234ze(E) employing a new experimental apparatus based on the transient hot wire (THW) technique (Wakeham et al., 1991). The measurements have been carried out in the temperature range between 243 K and 343 K at pressure up to 8 MPa and the results have been compared with the ones available in the literature. Also, the THW apparatus have been tested previously on toluene and the results are reported here.

Table 1
Material specification.

Chemical name	CAS number	Supply	Purity [molar fraction]
toluene	108-88-3	PanReac AppliChem	0.998
trans-1,3,3,3-tetrafluoropropene	1645-83-6	Honeywell	0.999

2. Experimental section

Table 1 reports the details for each of the samples used in this work. Each sample have been degassed through several freezing-pumping-thawing cycles.

The thermal conductivity measurements have been carried through the transient hot wire technique described in details by Wakeham et al. (1991). Fig. 1 shows the apparatus applied in this work. Fig. 2 shows a detailed view of the hot wire sensor, which is the core of the apparatus. The hot wire sensor consists of two wires made of Tantalum with a 25 μm diameter. The wires are 21.34 mm and 49.56 mm long, respectively. Except for their length, which is different to compensate for the end effects with respect to the theoretical infinite wire (Assael et al., 2004, 2010), the two wires are identical and connected together one over the other to be in the most similar conditions during the measurements. During the operation, a 46.6 cm^3 stainless steel pressure cell is first filled with the sample from the sample bottle up to a pressure above the saturation pressure of the fluid at the highest temperature in the circuit, in order to ensure that the wires are totally immersed. The pressure cell is placed in a vessel filled with a secondary fluid and its temperature is controlled by an external thermostatic bath with a stability of 0.02 K. As secondary fluid, water was employed for the measurements from 343 K to 283 K, while ethanol (CAS No. 64-17-5) was used for the measurements from 273 K to 243 K. An handpump is connected to the pressure cell through a 1/16″ (internal diameter) stainless steel tube and it is used to regulate the pressure. The experimental temperature is measured by means of a PT100Ω placed in the vessel and in contact with the external wall of the pressure cell. Such sensor is connected to an Agilent 34970 A multimeter to convert

Table 2
Experimental thermal conductivity for toluene and thermal conductivity calculated with Refprop 10.0. The subscripts *exp* and *ref* refer to the experimental data and the thermal conductivity calculated with Refrop 10.0 software, respectively.

T [K]	λ_{exp} [mW m^{-1} K^{-1}]	λ_{ref} [mW m^{-1} K^{-1}]	$\frac{\lambda_{exp}-\lambda_{ref}}{\lambda_{exp}}$ [%]
294.15	130.58	131.50	−0.71
294.15	130.56	131.50	−0.73
294.15	130.51	131.50	−0.76
294.15	130.55	131.50	−0.73
294.15	130.54	131.50	−0.74
294.15	130.42	131.50	−0.83
294.15	130.47	131.50	−0.79
294.15	131.06	131.50	−0.34
294.15	130.90	131.50	−0.46
294.15	130.94	131.50	−0.43
309.15	126.57	127.35	−0.62
309.15	126.54	127.35	−0.64
309.15	126.57	127.35	−0.61
282.15	132.39	134.81	−1.82
282.15	132.62	134.81	−1.65
282.15	132.47	134.81	−1.77
282.15	132.45	134.81	−1.78
282.15	132.42	134.81	−1.80
282.15	133.09	134.81	−1.29
282.15	133.00	134.81	−1.36
324.15	122.34	123.20	−0.70
324.15	122.38	123.20	−0.67
324.15	122.49	123.20	−0.57
324.15	122.76	123.20	−0.36
324.15	122.81	123.20	−0.31
324.15	122.88	123.20	−0.25

the signal in temperature values. The temperature sensor was calibrated in the temperature range between 223.15 K and 423.15 K, with an accuracy of 0.05 K. Considering the temperature stability recorded for the bath, the temperature uncertainty is estimated to be 0.07 K. The pressure is measured by a Druck PMP 4070 pressure transducer with a 13.5 MPa FS and an accuracy of 0.04% FS. The THW instrument, which measures the thermal conductivity, is a TWH-01L model developed by Accuintruments. The measure is based on the elaboration of the signal provided by a Wheatstone bridge in which two branches include one of the two hot wire sensors, so that the bridge is sensitive to the difference in the resistance of the two wires. The signal from the THW instrument is acquired and elaborated by a dedicated software. The instrumentation provided by Accuinstruments consisted in the two pressure vessels, the TWH sensor and the HW controller/data reader (see Fig. 1 for reference). The apparatus was completed by the authors with the temperature and pressure sensors and controllers (thermostatic bath and handpump) and the tubing. Moreover, the external vessel was further insulated with 1 cm of nitrile butadiene rubber (NBR) all around the volume and 5 cm of expanded sintered polystyrene (EPS) on the top and the bottom of the cell, in order to minimize the thermal dispersion, which can influence the measurement.

After the evacuation through a vacuum pump, the sample was sent into the apparatus in the vapor phase filling all the tubing and the handpump piston which was at the bottom of the run. Then, monitoring the pressure and the temperature, the sample was compressed through the handpump until it became liquid. The measurements were carried out along isotherms and the pressure was set through the handpump, recording at least three replicants for each temperature-pressure set-point. Once temperature and pressure reached the equilibrium, one thermal conductivity point was measured. Since the measurement itself slightly disturbed the thermal equilibrium inside the cell by warming up the hot wire sensor, each replicant was measured after at least 15 min from the previous one.

Table 3
Experimental thermal conductivity for R1234ze(E) and thermal conductivity calculated with Refprop 10.0. The subscripts *exp* and *ref* refer to the experimental data and the thermal conductivity calculated with Refrop 10.0 software, respectively.

T [K]	p [MPa]	λ_{exp} [mW m^{-1} K^{-1}]	λ_{ref} [mW m^{-1} K^{-1}]	$\frac{\lambda_{exp}-\lambda_{ref}}{\lambda_{exp}}$ [%]
283.15	0.996	80.02	79.88	0.18
283.15	1.986	80.68	80.51	0.21
283.15	4.006	81.87	81.76	0.14
283.15	5.993	82.78	82.93	−0.18
283.15	8.001	83.84	84.07	−0.28
302.89	1.237	73.77	73.12	0.88
302.89	2.049	73.95	73.74	0.29
302.89	4.008	75.14	75.15	−0.01
302.89	6.006	76.30	76.52	−0.28
302.89	8.021	77.78	77.82	−0.06
322.81	2.022	67.22	67.08	0.21
322.81	4.000	69.89	68.82	1.54
322.81	6.003	71.05	70.44	0.87
322.81	8.009	71.46	71.94	−0.67
342.64	3.994	63.44	62.77	1.06
342.66	6.012	63.01	64.75	−2.76
342.67	8.011	64.51	66.52	−3.13
342.67	4.008	62.38	62.76	−0.60
293.14	1.223	76.12	76.52	−0.52
293.14	2.007	76.64	77.06	−0.55
293.13	3.995	78.04	78.38	−0.44
293.14	6.009	79.24	79.66	−0.53
293.14	8.005	80.02	80.87	−1.07
312.82	2.009	70.13	70.38	−0.36
312.89	3.494	71.37	71.54	−0.23
312.89	6.004	74.35	73.41	1.26
312.88	8.005	73.93	74.80	−1.18
332.79	2.005	63.74	63.76	−0.03
332.81	4.010	64.24	65.75	−2.35
332.79	6.017	66.60	67.54	−1.41
332.79	8.070	68.06	69.21	−1.69
332.78	3.996	66.64	65.74	1.35
273.74	1.206	82.82	83.45	−0.76
273.76	2.008	84.16	83.89	0.32
273.74	4.030	84.70	85.09	−0.46
273.74	5.998	85.99	86.18	−0.21
273.74	8.003	87.49	87.25	0.28
264.13	1.193	88.04	86.99	1.19
264.13	2.013	88.87	87.44	1.61
264.13	4.008	88.93	88.51	0.47
264.13	6.003	89.33	89.55	−0.24
264.13	8.010	90.83	90.56	0.30
254.47	2.021	92.30	91.04	1.36
254.47	4.003	92.38	92.03	0.38
254.47	5.982	94.16	93.00	1.24
254.47	8.018	93.82	93.97	−0.15
243.29	2.014	97.18	95.37	1.87
243.30	4.004	96.77	96.25	0.53
243.30	6.002	96.15	97.16	−1.05
243.30	8.023	97.20	98.05	−0.88

2.1. Uncertainty analysis

The combined uncertainty in the thermal conductivity was calculated by means of Eq. (1).

$$\frac{u(\lambda)}{\lambda} = \sqrt{u_0^2(\lambda) + \left(\frac{\sigma(\lambda)}{\lambda}\right)^2 + \left(\frac{\partial\lambda}{\partial T}\frac{u(T)}{\lambda}\right)^2 + \left(\frac{\partial\lambda}{\partial p}\frac{u(p)}{\lambda}\right)^2} \quad (1)$$

where $u(\theta)$ denotes the uncertainty on the measured quantity θ. λ, T and p are the measured thermal conductivity, temperature and pressure, respectively. $u_0(\lambda)$ represents the uncertainty on the thermal conductivity provided by the aforementioned dedicated software and declared by the instrument constructor to be equal to ±1%. Such uncertainty takes into account parameters such as the voltage applied to the Wheatstone bridge and the measurement of the experimental time, but it does not consider the measurement of temperature and pressure. $\sigma(\lambda)$ represents the standard deviation in the measured thermal conductivity

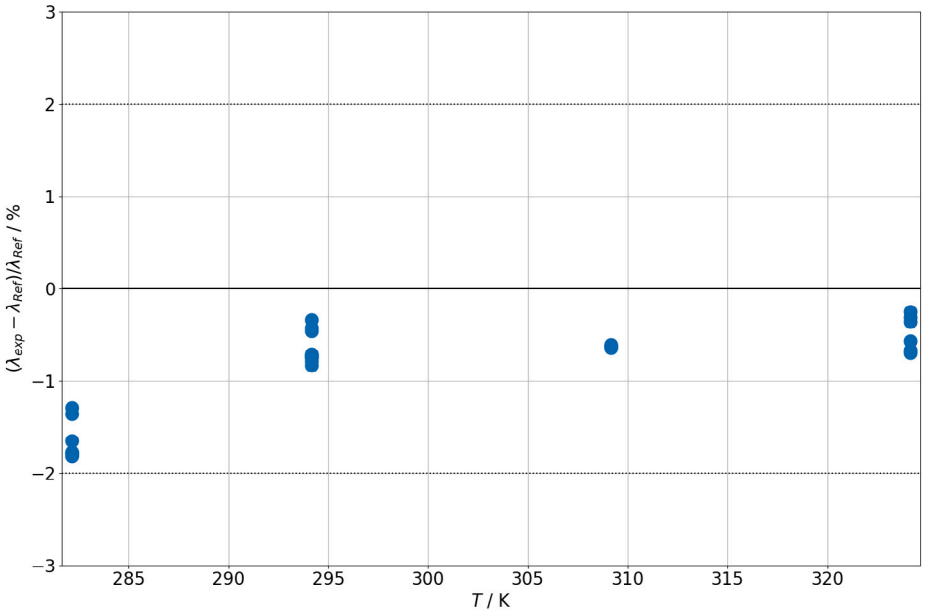

Fig. 3. Deviations of thermal conductivity experimental data with respect to Refprop 10.0 software for toluene.

among the replicated measurements of a single point. The terms $\frac{\partial\lambda}{\partial T}u(T)$ and $\frac{\partial\lambda}{\partial p}u(p)$ represent the sensitivity of the thermal conductivity to the temperature and pressure, respectively, were calculated as Eqs. (2)–(3):

$$\frac{\partial\lambda}{\partial T}u(T) = \lambda^{RP}(T,p) - \lambda^{RP}(T+u(T),p) \quad (2)$$

$$\frac{\partial\lambda}{\partial p}u(p) = \lambda^{RP}(T,p) - \lambda^{RP}(T,p+u(p)) \quad (3)$$

where λ^{RP} is the thermal conductivity calculated through Refprop 10.0 software (Lemmon et al., 2018). The temperature and pressure uncertainties $u(T)$ and $u(p)$ take into account both the accuracy of sensors and the stability of temperature and pressure along the measurement of a single thermal conductivity point.

The terms $u_0(\lambda)$ and $\sigma(\lambda)$ contributed the most to the overall combined uncertainty, while the terms $\frac{\partial\lambda}{\partial T}u(T)$ and $\frac{\partial\lambda}{\partial p}u(p)$ gave only a marginal contribution (less than 0.1%). Under these assumptions, an expanded uncertainty (k = 2) on the thermal conductivity within 2% was estimated.

3. Results

In order to verify the accuracy of the new thermal conductivity apparatus, 26 points have been measured for toluene at temperatures around 281 K, 293 K, 308 K and 323 K at atmospheric pressure. The results are reported in Table 2. Then, the thermal conductivity data for toluene have been compared with the Extended Corresponding State (ECS) model implemented in Refprop 10.0 (Lemmon et al., 2018). Such correlation is given with an uncertainty of 2% along the saturation curve and less than 3% for pressures up to 700 MPa and temperatures up to 550K. The comparison is shown in Fig. 3 and the deviations resulted to be always within 2% with respect to Refprop 10.0.

After the verification process with toluene, 50 thermal conductivity data have been measured for R1234ze(E) in the compressed liquid region in the temperature range from 243 K and 343 K and from pressure close to saturation and up to 8 MPa. Table 3 reports the measured data. Fig. 4 shows the distribution of the data measured in the present work with respect to the open literature data for the thermal conductivity of R1234ze(E). Fig. 5 reports the measured thermal conductivity data as a function of the density. Such properties have been calculated through Refprop 10.0 (Lemmon et al., 2018) with the experimental temperature and pressure as inputs. For R1234ze(E), Refprop 10.0 implements the EoS by Thol and Lemmon (2016) for the density and the ECS model by Perkins and Huber (2011) for the thermal conductivity.

4. Discussion

Figs. 6 and 7 compare the deviations between the experimental thermal conductivity data measured in this work and the ones reported by Perkins and Huber (2011) and Miyara et al. (2011) with respect to the correlation implemented in Refprop 10.0 as a function of temperature and pressure, respectively. The data reported by Perkins and Huber (2011) in both liquid and vapor phase are the only ones which have been used to develop the correlation implemented in Refprop 10.0 software with a declared uncertainty of 1% for the liquid phase and 2% for the vapor phase. In the same paper, the other datasets have been compared to such correlation resulting in a good agreement with the data of Miyara et al. (2011), while deviations greater than 20% have been reported for all the data of Grebenkov et al. (2009), which, for this reason, are not reported in Figs. 6–7.

The data reported in this work show a bias of 0.15% and an AAD of 0.83% with respect to Refprop 10.0. It is worth to notice that 4 points out of 50 present an absolute deviation between 2% and 3% with respect to the reference correlation. These points have been measured at temperatures greater than 320 K where a higher thermal dispersion was observed. It was observed that the temperature fluctuations was within ±0.01 K for each isotherm. A reason for the higher deviations of some high temperature data can be found in a non-uniform thermal loss along the vessel, which might have led to slight convective motions inside the pressure cell. Thus, further developments of the apparatus will involve the thermal insulation of the thermostatic liquid vessel.

5. Conclusions

This work presents the results of thermal conductivity measurements on R1234ze(E). The experimental campaign has been carried out by means of a transient hot-wire apparatus in the compressed liquid region in the temperature range between 243 K and 343 K at pressures

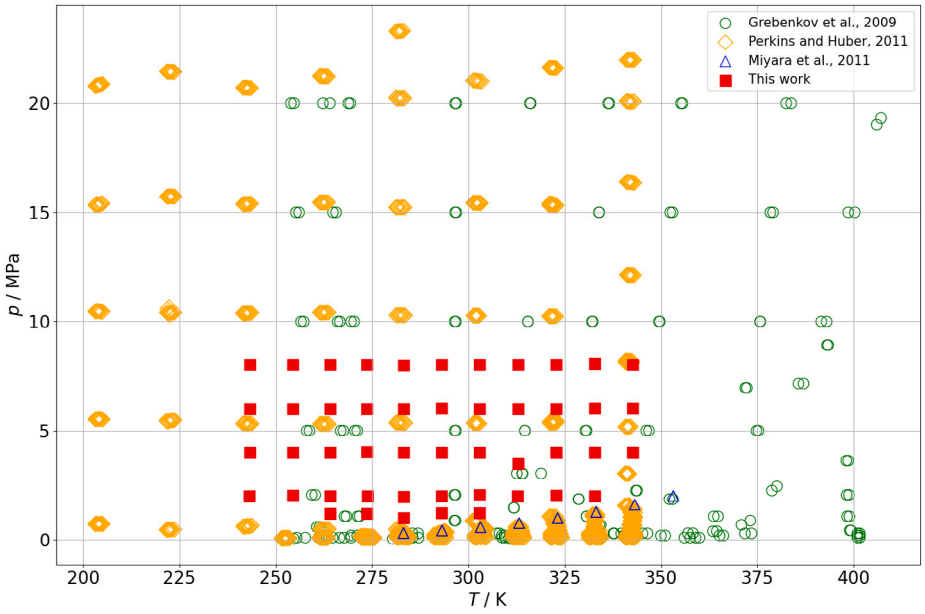

Fig. 4. Pressure and temperature distribution of the thermal conductivity presented in this work compared to the open literature.

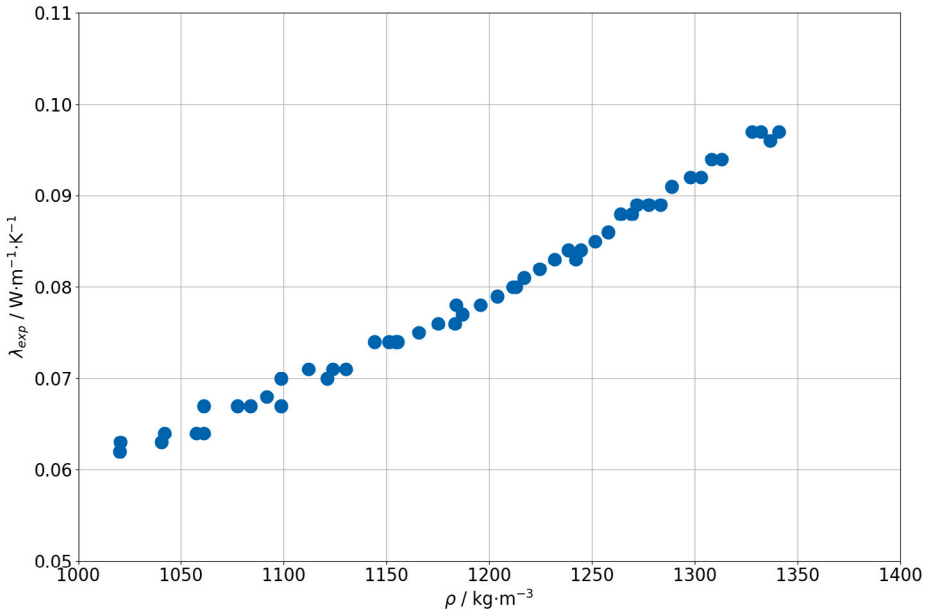

Fig. 5. Experimental thermal conductivity data as a function of density. The density was calculated with Refprop 10.0 (Lemmon et al., 2018) considering the EoS by Thol and Lemmon (2016).

from 1 MPa to 8 MPa, resulting in 50 experimental points. Considering the verification of the experimental apparatus previously carried out on toluene, the uncertainty on the thermal conductivity was estimated to be equal to 2%. The measurements have been compared with the ECS model implemented in Refprop 10.0 and developed by Perkins and Huber (2011). An AAD of 0.83% has been calculated and only 4 points, at temperatures higher than 320 K, resulted to have an absolute deviation greater than 2%. Such higher deviations can be attributed to the non uniform thermal losses of the vessel in which the pressure vessel was immersed in the thermostatic bath, thus further development will be carried out on the thermal insulation of the thermostatic liquid vessel.

Declaration of competing interest

The authors declare that they have no known competing financial interests or personal relationships that could have appeared to influence the work reported in this paper.

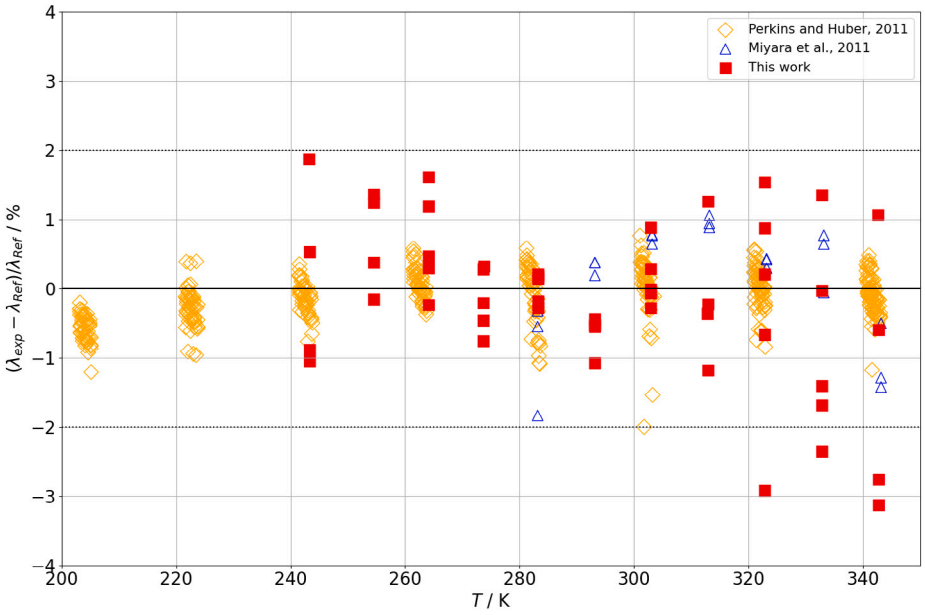

Fig. 6. Deviations of thermal conductivity experimental data with respect to Refprop 10.0 software for R1234ze(E) as a function of temperature.

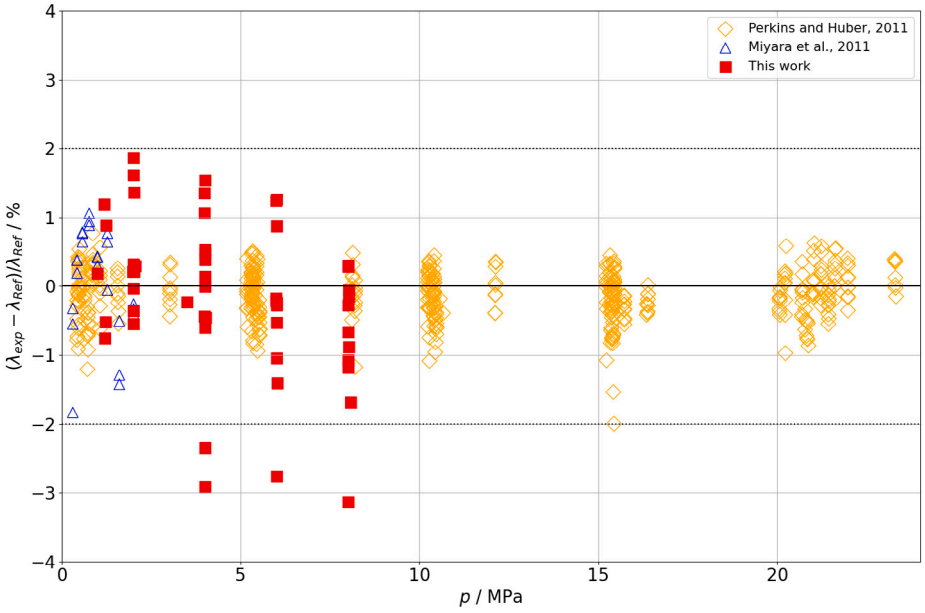

Fig. 7. Deviations of thermal conductivity experimental data with respect to Refprop 10.0 software for R1234ze(E) as a function of pressure.

References

Assael, M.J., Antoniadis, K.D., Wakeham, W.A., 2010. Historical evolution of the transient hot-wire technique. Int. J. Thermophys. 31, 6.

Assael, M.J., Chen, C.F., Metaxa, I., Wakeham, W.A., 2004. Thermal conductivity of suspensions of carbon nanotubes in water. Int. J. Thermophys. 25, 4.

Bobbo, S., Nicola, G., Zilio, C., Brown, J., Fedele, L., 2018. Low GWP halocarbon refrigerants: A review of thermophysical properties. Int. J. Refrig. 90, 181–201. http://dx.doi.org/10.1016/j.ijrefrig.2018.03.027.

European Commission, 2014. Regulation (EU) No 517/2014 of the European Parliament and of the Council of 16 2014 on fluorinated greenhouse gases and repealing Regulation (EC) No 842/2006 Text with EEA relevance. https://eur-lex.europa.eu/eli/reg/2014/517/oj.

Fedele, L., Lombardo, G., Greselin, I., Menegazzo, D., Bobbo, S., 2023. Thermophysical properties of low GWP Refrigerants: An Update. Int. J. Thermophys. 44. http://dx.doi.org/10.1007/s10765-023-03191-5.

Grebenkov, A., Hulse, R., Pham, H., Singh, R., 2009. Physical properties and equation of state for trans-1, 3 3, 3-tetrafluoropropene. In: Proc. 3rd IIR Conference on Thermophysical Properties and Transfer Processes of Refrigerants. Boulder, CO, USA.

Invernizzi, C., Iora, P., Preißinger, M., Manzolini, G., 2016. HFOs as substitute for R-134a as working fluids in ORC power plants: A thermodynamic assessment and thermal stability analysis. Appl. Therm. Eng. 103, 790–797. http://dx.doi.org/10.1016/j.applthermaleng.2016.04.101.

IPCC, 2021. Climate Change 2021. The Physical Science Basis: the Working Group I contribution to the Sixth Assessment Report of the Intergovernmental Panel on Climate Change, https://www.ipcc.ch/report/ar6/wg1.

Kondou, C., Koyama, S., 2015. Thermodynamic assessment of high-temperature heat pumps using low-GWP HFO refrigerants for heat recovery. Int. J. Refrig. 53, 126–141. http://dx.doi.org/10.1016/j.ijrefrig.2014.09.018.

Lemmon, E.W., Bell, I.H., Huber, M.L., McLinden, M.O., 2018. NIST Standard Reference Database 23: Reference Fluid Thermodynamic and Transport Properties-REFPROP,

Version 10.0, National Institute of Standards and Technology. https://www.nist.gov/srd/refprop.

Makhnatch, P., Khodabandeh, R., 2014. The role of environmental metrics (GWP, TEWI, LCCP) in the Selection Of Low GWP Refrigerant. Energy Procedia 61, 2460–2463. http://dx.doi.org/10.1016/j.egypro.2014.12.023.

McLinden, M., Kazakov, A., Brown, J., Domanski, P., 2014. A thermodynamic analysis of refrigerants: Possibilities and tradeoffs for Low-GWP refrigerants. Int. J. Refrig. 38, 80–92. http://dx.doi.org/10.1016/j.ijrefrig.2013.09.032.

Miyara, A., Fukuda, R., Tsubaki, K., 2011. Thermal conductivity of saturated liquid of R1234ze(E)+R32 and R1234yf+R32 mixtures. In: Proc. 23rd IIR International Congress of Refrigeration. Prague, Czech Republic.

Mota-Babiloni, A., Navarro-Esbrí, J., Molés, F., Cervera, A., Peris, B., Verdú, G., 2016. A review of refrigerant R1234ze(E) recent investigations. Appl. Therm. Eng. 95, 211–222. http://dx.doi.org/10.1016/j.applthermaleng.2015.09.055.

Perkins, R., Huber, M., 2011. Measurement and Correlation of the Thermal Conductivity of 2 3, 3 3-Tetrafluoroprop-1-ene (R1234yf) and trans-1, 3 3, 3-Tetrafluoropropene (R1234ze(E)). J. Chem. Eng. Data 56, 4868–4874.

Thol, M., Lemmon, E., 2016. Equation of State for the Thermodynamic Properties of trans-1, 3 3, 3-Tetrafluoropropene [R-1234ze(E)]. Int. J. Thermophys. 37. http://dx.doi.org/10.1007/s10765-016-2040-6.

United Nations Environment Programme, 2016. The Kigali Amendment to the Montreal Protocol: HFC Phase-down. https://wedocs.unep.org/20.500.11822/26589.

Wakeham, W., Sengers, J., Nagashima, A., 1991. Measurement of the transport properties of fluids. Meas. Transp. Prop. Fluids.